21st Australasian Fluid Mechanics Conference
Adelaide, Australia
10-13 December 2018

Periodicity of large-scale coherence in turbulent boundary layers

C. M. de Silva[1], D. Chandran[1], R. Baidya[1], N. Hutchins[1] and I. Marusic[1]

[1] Department of Mechanical Engineering, The University of Melbourne, Victoria 3010, Australia.

Abstract

This study examines the pronounced periodicity of large-scale coherent structures in turbulent boundary layers, which are of the order of the boundary layer thickness and reside in the logarithmic and wake regions. To this end, a series of multi-camera planar particle image velocimetry (PIV) measurements are conducted in a streamwise-spanwise and streamwise-wall normal arrangements at a friction Reynolds number of $Re_\tau \approx 2500$. The experiments are configured to capture velocity fields that cover a streamwise extent in excess of 15 boundary layer thicknesses. Preliminary observations of the vector fields reveal large-scale streamwise and spanwise organisation instantaneously, which is often lost when only examining mean statistics. By extracting the dominant streamwise and spanwise Fourier modes of the large-scale motions, a clearer picture of these structural organisations and coherence is presented. Further, through targeted inspection of these δ-scaled modes we observe that these features extend across significant wall-normal extents and only a fraction of these modes appear to have coherence that extends to the wall. Collectively, these findings are likely to inform future attempts in modelling the representative structures in turbulent boundary layers due to the persistent presence of these recurrent instantaneous regions of large-scale coherence.

Introduction

The structural composition of turbulent boundary layers has been the subject of many investigations over the last half a century (see [5] for a recent review). A large number of these studies have shown that the flow is populated by recurrent turbulent structures, commonly referred to as 'coherent structures'. Of particular interest in the present study is to capture instantaneous snapshots of large-scale structures that are of the order of the boundary layer thickness, which are known to inhabit the log and outer regions of boundary layers at moderate to high Reynolds number. Prior evidence of these structures has largely been provided by inferring spatial information from temporally resolved single-component point measurements using Taylor's frozen turbulence hypothesis [4]. However, this technique is limited, particularly over large spatial extents [2]. More recently, direct numerical simulations with large spatial domains [9] have provided insight into these structures. Measurements using particle image velocimetry (PIV) with large spatial domains such as those presented herein, offer a promising approach to examine these large-scale motions.

One distinct feature reported in the large-scale coherence in turbulent boundary layers is the pronounced periodicity of the large-scale coherent structures in turbulent boundary layers. These structures have been reported to be in the order of the boundary layer thickness and reside in the logarithmic and wake regions [3]. This behaviour is best described with reference to figure 1(a), which shows a representative snapshot of the streamwise velocity fluctuations, u, from the present PIV experiments on a streamwise wall-normal plane. Here, the boundary layer thickness, δ, corresponds to the wall distance where the mean streamwise velocity is 99% of the free-stream velocity, U_∞. From this velocity field, it is clear that the positive and negative u coherence appears to have some pronounced degree of periodicity at a particular wavelength (regions encapsulated by the ellipses), which is often lost when only examining mean statistics. Similar periodic patterns have also been observed on the wall-parallel plane of a boundary layer. In particular, the near-wall region ($z^+ \approx 15$) is thought to be composed of streaky patterns of positive and negative u coherence with a characteristic spanwise spacing of approximately 100 viscous wall units [6]. Past works using PIV measurements confirmed that these patterns are also present further away from the wall and appear to scale with wall-distance (see [10]). However, their true spatial extent is usually not captured.

Accordingly, in the present work, a series of multi-camera particle image velocimetry (PIV) measurements are conducted in a planar arrangement, which are configured to capture non-simultaneous velocity fields on streamwise/wall-normal and streamwise/spanwise planes that cover a streamwise extent in excess of 15δ, allowing us to capture the full extent of the larger coherent motions that are present in the boundary layer (see figure 1a).

Throughout this work, the coordinate system x, y and z refer to the streamwise, spanwise and wall-normal directions, respectively. Corresponding instantaneous streamwise, spanwise and wall-normal velocity fluctuations are represented by u, v and w. Overbars denote average quantities and the superscript + refers to normalisation by viscous variables. For example, we use $u^+ = u/U_\tau$ for velocity, where U_τ is the friction velocity.

Description of experiments

The experiments described in this paper are performed in the High Reynolds Number Boundary Layer Wind Tunnel (HRNBLWT) at the University of Melbourne. The tunnel consists of a large development length of approximately 27m, offering the capability of achieving high Reynolds numbers at relatively low freestream velocities. The present campaign is tailored to obtain snapshots of very large scale streamwise motions with sufficient fidelity. Hence, experiments are conducted near the upstream end of the test section ($x \approx 4$ m) where the boundary layer thickness is $\delta \approx 90$ mm. This enables us to capture well resolved instantaneous snapshots at moderate Reynolds numbers with a streamwise extent in excess of 15δ. To achieve this, the field of view (FOV) is constructed by stitching the imaged region from eight high-resolution 14 bit PCO 4000 PIV cameras. Two camera arrangements are employed (see figure 2); one to quantify velocity fields on a large streamwise/wall-normal plane and the other on a streamwise/spanwise plane, hereafter referred to as SW and WP database, respectively. The red solid lines in figures 2(a) and (b) show the combined field of view for each arrangement. Table 1 details the key experimental parameters for both arrangements.

Measurements for both planes are conducted at a freestream velocity of 10 m/s, with corresponding Reynolds number across the FOV of $Re_\tau \approx 2400-2900$. The WP database is acquired at a wall-normal location of $x/\delta \approx 0.4$. The image pairs are processed using an in-house PIV package, with the final window sizes for each dataset summarised in table 1. Further details on the measurements can be found in [1].

Results

Dominant energetic modes

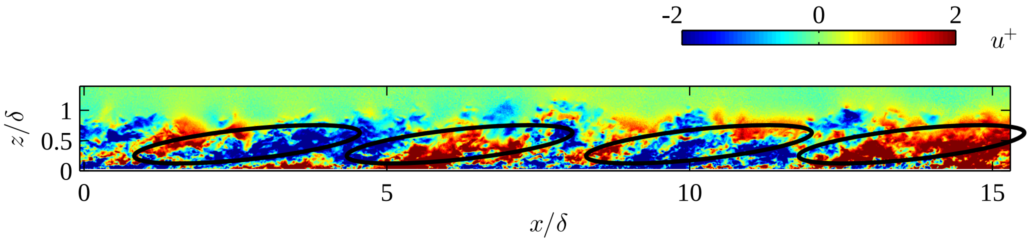

Figure 1: (a) Instantaneous velocity field from the PIV datasets at $Re_\tau \approx 2500$. Results are presented on a streamwise/wall normal plane and the colour contours represent the instantaneous streamwise velocity fluctuations u. Spatial extents are normalised by the boundary layer thickness δ. Regions encapsulated by the solid ellipses highlights coherent regions of alternating positive (red) and negative (blue) u that exhibit periodicity at a particular wavelength.

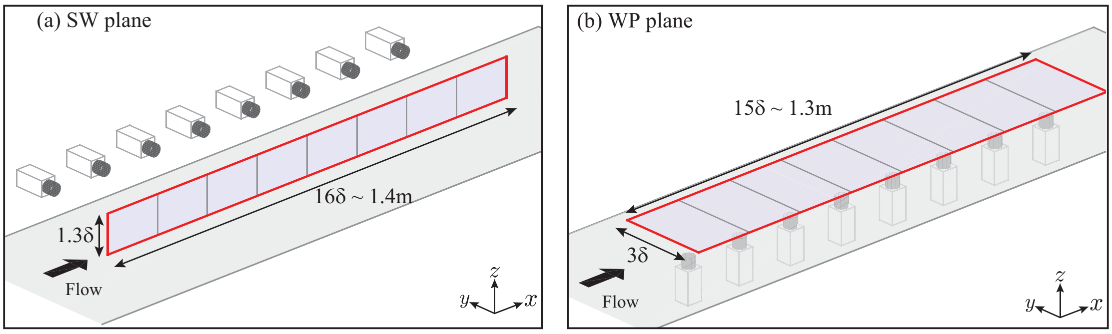

Figure 2: Experimental setup used to conduct large field of view planar PIV experiments in the HRNBLWT. (a) and (b) shows the configuration used to capture a streamwise/wall-normal plane and streamwise/spanwise plane, respectively. The red solid line corresponds to the combined field of view captured from the multi-camera imaging system.

Plane	U_∞	Re_τ	z	ν/U_τ	Window size	
	(m/s)		location	(μm)	l^+	pixels
SW	10	2500	-	42	26	32×32
WP	10	2500	$z\approx0.4\delta$	42	50	32×32

Table 1: Summary of experimental parameters. The interrogation window size corresponds to the number of pixels used for PIV cross-correlation. The friction velocity U_τ is computed at the middle of the FOV using the method outlined in [7].

The large spatial extent of the present databases allows us to capture any periodicity in the large-scales present in the flow. However, these features, that are generally readily visible on the instantaneous velocity fields (see figure 1), are not evident in the time-averaged statistics (see [9] for recent results). This is likely the result of the statistical smearing that is caused by the superposition of the wide range of energetic scales present in turbulent boundary layers, which masks the periodic patterns of the streamwise or spanwise coherence. Therefore, in order to sort the dominant energetic modes or scales, we perform a sorting technique similar to that proposed by [3].

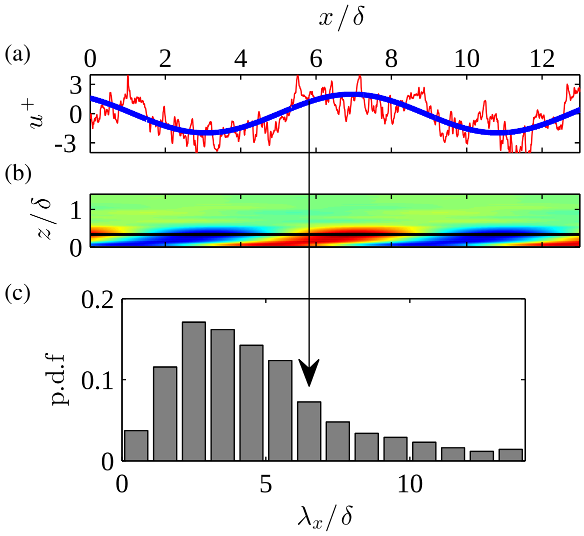

Figure 3: (a) Streamwise trace of the u fluctuation extracted at $z/\delta \approx 0.4$ from the example shown in figure 1. The solid blue line shows the dominant streamwise Fourier mode. (b) The reconstructed u using only the dominant δ-scaled Fourier mode shown in (a). (c) Probability distribution of dominant streamwise Fourier modes at $z/\delta \approx 0.4$ from the SW database at $Re_\tau \approx 2500$.

More specifically, for the SW database, a Fourier decomposition is performed in x at each z location for energetic modes which are of order δ. To perform this, a streamwise trace of the u fluctuations is extracted from each frame at a prescribed reference height. As an example, the red line in figure 3(a) shows the signal extracted from the instantaneous velocity field shown previously in figure 1 at $z/\delta \approx 0.4$, while the blue line corresponds to the most dominant streamwise Fourier mode obtained from the signal. The corresponding velocity field for u for the dominant streamwise mode is presented in figure 3(b), where the phase is determined by performing a Fourier decomposition in x at each z location. It should be noted that even though the mode wavelength is prescribed here, the wall normal coherence and inclination is not (and comes about only due to the phase relationship between these modes). The PIV frames are then sorted or 'binned' based on the streamwise mode λ_x that carries the highest energy at that particular frame (see arrow in figure 3). In a similar fashion, for the WP databases, a Fourier decomposition is performed in both x and y, which allows us to extract the dominant modes in both the streamwise (λ_x) and spanwise (λ_y) directions.

Figure 3(c) presents a p.d.f of the dominant streamwise modes, λ_x, at $z/\delta \approx 0.4$ for the SW database at $Re_\tau \approx 2500$. For the chosen bin size here, which is of the order of δ, the results indicate that the instantaneous velocity fields exhibit periodicity over a range of streamwise wavelengths. However, the five most dominant periodic wavelengths account for ~70% of the frames

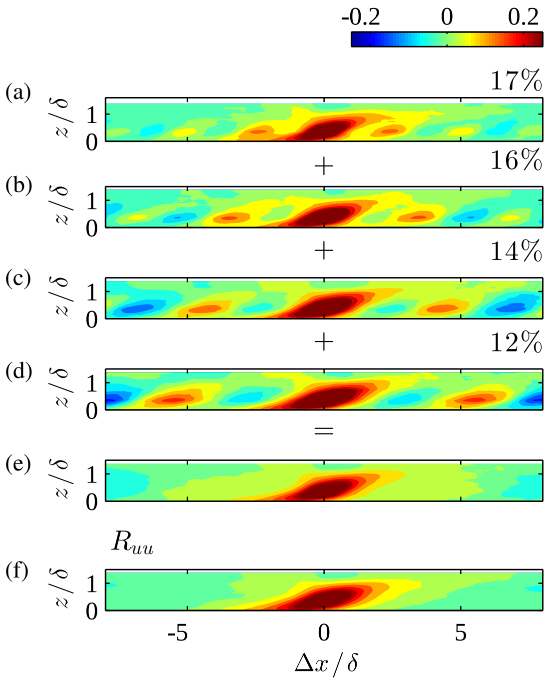

Figure 4: Colour contours of the two-point correlation function R_{uu} computed at reference location $z/\delta \approx 0.4$ for strongest dominant modes (a) $2 < \lambda_x/\delta < 3$, (b) $3 < \lambda_x/\delta < 4$, (c) $4 < \lambda_x/\delta < 5$ and (d) $5 < \lambda_x/\delta < 6$. (e) R_{uu} for the sum of the modes in (a-d), while (f) corresponds to the unconditioned R_{uu}.

when combined. The two-point correlations for the streamwise velocity fluctuations, R_{uu}, for the PIV frames that correspond to the four most common streamwise Fourier modes at $z/\delta \approx 0.4$ are shown in figures 4(a-d) for the SW database at $Re_\tau \approx 2500$. The results indicate that when the PIV frames are sorted in this fashion the two-point correlations clearly exhibit an underlying periodicity in the u coherence. This is expected at the reference height $z/\delta \approx 0.4$, however, our results reveal that these modes extend a considerable distance in the wall-normal direction in excess of 0.5δ and appear to exhibit a characteristic inclination angle which is not prescribed. It is worth noting that despite these repeating patterns describing most of the data, the superposition of these modes leads to an R_{uu} that exhibits no sign of periodicity (see figure 4e) and is similar to the unconditioned R_{uu} (figure 4f). Therefore, care must be taken when interpreting statistically averaged measures, such as R_{uu}, where instantaneous features can be masked. Furthermore, we note that even though our results reveal periodic patterns in the u coherence that have streamwise extents that span several δ, the true extent of some of these structures is likely to be larger due to their meandering nature [4].

In order to elucidate the three dimensional periodicity of the u coherence the same technique can be applied to the WP database in the spanwise direction. The results are presented in figure 5, which shows colour contours of R_{uu} for the four most common spanwise modes λ_y from the WP database at $Re_\tau \approx 2500$. The results exhibit an underlying periodicity for the u coherence that appears to extend for several δ in the streamwise direction. Further, our results confirm that these four modes account for over 80% of the PIV frames and once combined appear to recover the behaviour of the unconditioned R_{uu} (figures 5e and 5f).

Wall-normal coherence of periodic structures

Several past works have highlighted that a turbulent boundary layer is composed of a collection of structures that scale with distance from the wall. In particular, models described by Perry and co-workers (see [8]) based on the attached-eddy hypothesis have been shown to reasonably reproduce flow statistics of wall-bounded turbulence. These models propose that the boundary layer is composed of a collection of structures that scale with wall distance and are largely ‘attached’ or have coherence that extends to the wall. The SW database in the present work allows us to examine whether the large-scale periodic structures are coherent with the wall. This is illustrated in figure 6, where two instantaneous velocity fields (c.f. 6a and 6d) and the corresponding reconstructed u for the dominant δ-scaled Fourier modes (c.f. 6b and 6e) at a wall-normal height of $z/\delta = 0.4$, exhibit a distinct behaviour. More specifically, the dominant δ-scaled Fourier mode for the first field (figure 6b) appear to exhibit coherence that extends to the wall, while the dominant δ-scaled Fourier mode in figure 6e, computed at the same z/δ, appears to be incoherent with the wall.

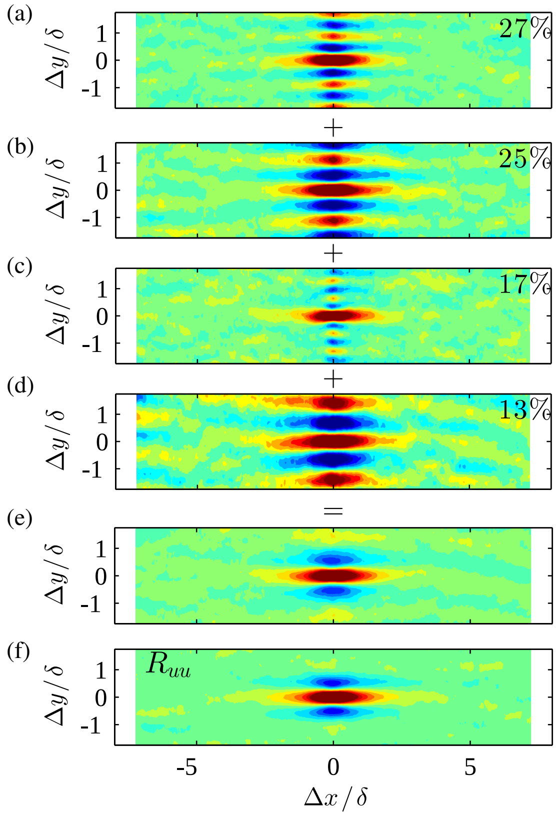

Figure 5: Colour contours of the two-point correlation function R_{uu} for strongest dominant spanwise modes, λ_y from the WP database at $z/\delta \approx 0.4$. (a) $0.75 < \lambda_y/\delta < 1$, (b) $1 < \lambda_y/\delta < 1.25$, (c) $0.5 < \lambda_y/\delta < 0.75$ and (d) $1.25 < \lambda_y/\delta < 1.5$. (e) R_{uu} for the sum of the modes in (a-d),while (f) corresponds to the unconditioned R_{uu}. Colour levels are same as in figure 4

In order to quantify this behaviour and attempt to compute the proportion of the dominant δ-scaled Fourier modes that are coherent with the wall (or ’attached’), a threshold is applied to the turbulence intensity of the dominant $O(\delta)$ modes, $\overline{u_s^2}$, (c.f. 6c and 6f). For the present case, the wall-normal extent of the Fourier modes is evaluated by setting a threshold equal to the freestream turbulence intensity (vertical dashed line in figures 6c and f). Figure 7 presents results for the fraction of ‘attached’ features as a function of wall-normal height once the aforementioned technique is applied to all the PIV frames of the SW database at $Re_\tau \approx 2500$. The results show that the proportion of ‘attached’ dominant λ-scaled streamwise Fourier modes decreases with wall-normal height. Interestingly, even in the logarithmic region of the flow (bounded by the vertical dashed lines), about 20% of the dominant δ-scaled periodic features appear to be incoherent with the wall. These observations are

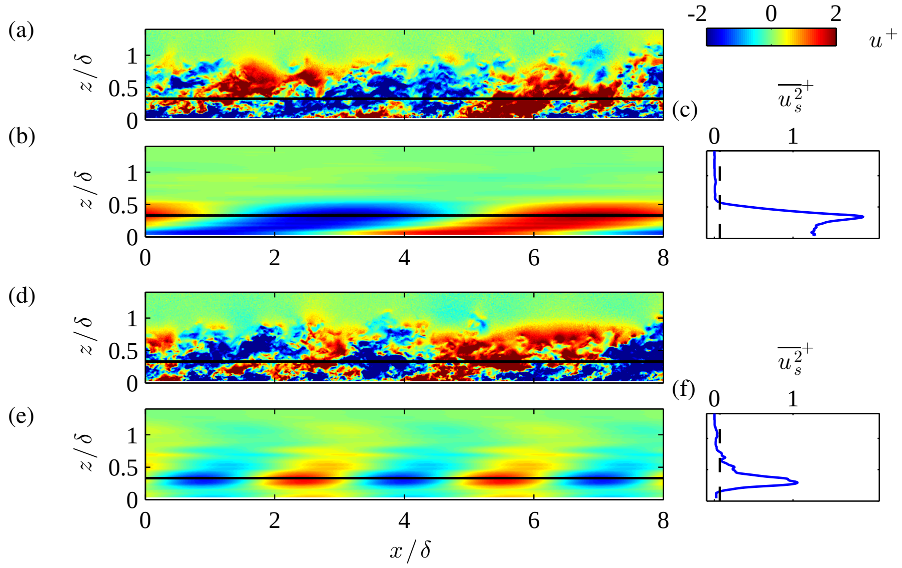

Figure 6: (a-c) Instantaneous velocity field where the dominant δ-scaled Fourier mode at $z/\delta \approx 0.4$ (shown in b) has coherence extending to the wall, 'attached'. (d-f) Instantaneous velocity field where the dominant δ-scaled Fourier mode at $z/\delta \approx 0.4$ (shown in e) does not have coherence that extends to the wall. (c,f) Streamwise turbulence intensity of the dominant δ-scaled Fourier mode ($\overline{u_s^2}$) as a function of z.

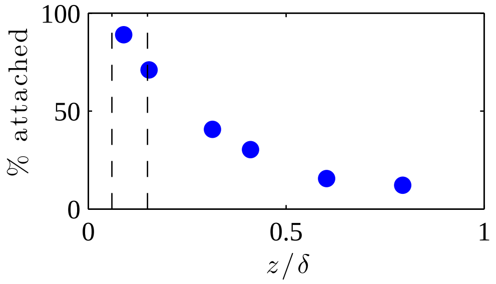

Figure 7: Percentage of attached dominant δ-scaled modes as a function of wall-normal location from the SW database at $Re_\tau \approx 2500$. The vertical dashed lines indicate the boundaries of the logarithmic region.

likely to have implications on the type of representative structures to be used in structure-based models for turbulent boundary layers, which are unlikely to be only purely a set of attached structures.

Conclusions

This paper examines the large-scale periodicity of the streamwise coherence in turbulent boundary layers. To this end, a set of multi-camera PIV measurements are described to capture a sufficiently large spatial domain in excess of ten times the boundary layer thickness. By extracting the dominant streamwise and spanwise Fourier modes of the large-scale motions we observe that instantaneously the *u* coherence exhibits periodic patterns that extend a considerable distance in the wall-normal direction and have inclination angles similar to those reported in previous works. Further, through targeted inspection of these δ-scaled modes we observe that only a fraction of these modes appear to have coherence that extends to the wall. These observations are likely to provide insight in modelling the representative structures of turbulent boundary layers and also have implications to flow control strategies of large-scale motions, where it may be possible to exploit these periodicities.

Acknowledgements

The authors wish to gratefully thank the financial support of the Australian Research Council.

[1] de Silva, C. M., Squire, D. T., Hutchins, N. and Marusic, I., Towards capturing large scale coherent structures in boundary layers using particle image velocimetry., in *Proc. 6th Aust. Conf. Laser Diag. Fluid Mech. Comb.*, University of Melbourne, 2015, 1–4, 1–4.

[2] Dennis, D. J. C. and Nickels, T. B., On the limitations of Taylor's hypothesis in constructing long structures in a turbulent boundary layer, *J. Fluid Mech.*, **614**, 2008, 197–206.

[3] Hutchins, N., Ganapathisubramani, B. and Marusic, I., Spanwise periodicity and the existence of very large scale coherence in turbulent boundary layers, in *Proc. 4th Turb. Shear Flow Phenom.*, 2018.

[4] Hutchins, N. and Marusic, I., Evidence of very long meandering features in the logarithmic region of turbulent boundary layers, *J. Fluid Mech*, **579**, 2007, 1–28.

[5] Jiménez, J., Coherent structures in wall-bounded turbulence, *J. Fluid Mech.*, **842**, 2018, P1.

[6] Kline, S. J., Reynolds, W. C., Schraub, F. A. and Runstadler, P. W., The structure of turbulent boundary layers, *J. Fluid Mech.*, **30**, 1967, 741–773.

[7] Nagib, H. M., Chauhan, K. A. and Monkewitz, P. A., Approach to an asymptotic state for zero pressure gradient turbulent boundary layers, *Phil. Trans. R. Soc. A*, **365**, 2007, 755–770.

[8] Perry, A. E. and Chong, M. S., On the mechanism of wall turbulence, *J. Fluid Mech*, **119**, 1982, 106–121.

[9] Sillero, J. A., Jiménez, J. and Moser, R. D., Two-point statistics for turbulent boundary layers and channels at Reynolds numbers up to $\delta^+ = 2000$, *Phys. Fluids*, **26**, 2014, 105109.

[10] Tomkins, C. D. and Adrian, R. J., Spanwise structure and scale growth in turbulent boundary layers, *J. Fluid Mech.*, **490**, 2003, 37–74.